

Hydrodynamic and Brownian Fluctuations in Sedimenting Suspensions

J. T. Padding^{1,2} and A. A. Louis¹

¹*Department of Chemistry, Cambridge University, Lensfield Road, Cambridge CB2 1EW, United Kingdom*

²*Schlumberger Cambridge Research, High Cross, Madingley Road, Cambridge CB3 0EL, United Kingdom*

(Received 6 September 2004; published 23 November 2004)

We use a mesoscopic computer simulation method to study the interplay between hydrodynamic and Brownian fluctuations during steady-state sedimentation of hard sphere particles for Peclet numbers (Pe) ranging from 0.1–15. Even when the hydrodynamic interactions are an order of magnitude weaker than Brownian forces, they still induce backflow effects that dominate the reduction of the average sedimentation velocity with increasing particle packing fraction. Velocity fluctuations, on the other hand, begin to show nonequilibrium hydrodynamic character for $Pe > 1$.

DOI: 10.1103/PhysRevLett.93.220601

PACS numbers: 05.40.-a, 47.11.+j, 47.20.Bp, 82.70.Dd

Exactly what happens when a collection of particles sediments through a viscous solvent is a very simple question to pose, but a remarkably difficult one to answer [1,2]. In a classic tour de force, Batchelor [3] showed that the average sedimentation velocity v_s of hard spheres (HS) of hydrodynamic radius a has a lowest order correction $v_s = v_s^0(1 - 6.55\phi)$ where ϕ is the HS volume fraction and v_s^0 is the Stokes sedimentation velocity of a single sphere [1]. This substantial correction to v_s^0 with a volume fraction is caused by many-body hydrodynamic backflow effects that greatly complicate efforts to extend the Batchelor result to higher order in ϕ . Even less is understood about the velocity fluctuations around the average, $\delta v = v - v_s$. Using straightforward physical arguments, Caffish and Luke [4] predicted that for sedimentation these should diverge as $\langle(\delta v)^2\rangle \sim L$, where L is the smallest container size. This surprising result provoked a flurry of experimental and theoretical studies (see Ref. [2] for a review). Although it is agreed that hydrodynamic velocity fluctuations are relatively large, there is no consensus on the reasons (if any) for the purported breakdown of the Caffish-Luke argument at large L .

In addition to the fundamental interest and myriad applications of sedimentation itself, researchers have been motivated to investigate this problem because of its relevance to nonequilibrium statistical mechanics. Recent studies in this line include a theoretical prediction of a continuous nonequilibrium noise-driven phase transition between screened and unscreened phases [5], and an experimental study predicting a noise-induced effective “temperature” that could aid in developing an ensemble based statistical mechanics for driven systems [6].

Most theoretical studies of sedimentation have focused on the limit where Brownian forces are negligible, and only hydrodynamic interactions (HI) contribute. In other words, the dimensionless Peclet number

$$Pe = \frac{v_s^0 a}{D_{col}}, \quad (1)$$

which measures the relative strength of HI and Brownian forces, was assumed to be infinite. Here D_{col} is the equilibrium self-diffusion constant of the particles. When the gravitational energy gained by a particle sedimenting over a distance of one radius a is equal to the reduced temperature $k_B T$, then $Pe = 1$ [2], a criterion used to define the start of the colloidal regime [1]. Sedimentation at $Pe \leq 1$ has many important applications for colloidal dispersions, as well as for centrifugal diagnostic techniques commonly used for biological macromolecules [1].

In this Letter, we employ a recently proposed mesoscopic simulation method [7] to investigate steady-state sedimentation at finite Pe, where Brownian and HI both contribute to velocity fluctuations. To our knowledge, this problem has not been investigated in detail before. For all Pe studied, we find that the average sedimentation velocity is completely dominated by HI, even when they are much smaller than the Brownian forces. On the other hand, we argue that short time velocity fluctuations are dominated by Brownian forces up to surprisingly large Pe, while long-time fluctuations have predominantly hydrodynamic character even at moderate Pe.

To perform the simulations, we adapt stochastic rotation dynamics (SRD) [7] to the problem of sedimenting HS. SRD is a particle based method similar in spirit to the lattice Boltzmann model (LB), which has been extensively applied to sedimentation [8]. In contrast to LB, it naturally includes Brownian noise (see, however, [9]). In SRD a fluid is represented by N_f ideal particles of mass m_f . After propagating the particles for a time Δt_c , the system is partitioned into cubic cells of volume a_0^3 . The velocities relative to the center of mass velocity of each separate cell are rotated over a fixed angle around a random axis. This procedure conserves mass, momentum, and energy, and yields the correct hydrodynamic (Navier-Stokes) equations, *including* the effect of thermal noise [7]. The fluid particles only interact with each other through the rotation procedure, which can be viewed as a coarse graining of particle collisions over time and space. For this reason, the particles should not be inter-

preted as individual molecules but rather as a Navier-Stokes solver that naturally includes Brownian noise.

The colloid-colloid (cc) and colloid-fluid (cf) interactions are modeled by a repulsive potential: $\beta V_{ci}(r) = 10[(\sigma_{ci}/r)^{2n} - (\sigma_{ci}/r)^n + 1/4]$ ($r \leq 2^{1/n}\sigma_{ci}$). For $V_{cc}(r)$, $n = 24$, which should approximate HS behavior. For $V_{cf}(r)$ we set $n = 6$ and $\sigma_{cf} = 0.465\sigma_{cc}$, slightly below half the colloid diameter σ_{cc} , which allows for lubrication. These potentials result in a hydrodynamic radius $a \approx 0.8\sigma_{cf}$. Colloid-colloid and colloid-fluid forces are integrated with a standard velocity Verlet molecular dynamics integrator with a time step $t = \frac{1}{4}\Delta t_c$ [10].

We now briefly discuss our choice of SRD parameters; a more detailed account will be published elsewhere [11]. The kinematic viscosity $\nu = \eta_f/\rho_f$, where η_f is the viscosity and ρ_f the mass density of the fluid, is an important parameter because it sets the time scale over which the momentum (vorticity) diffuses away. In dimensionless form it is desirable to have $\nu/D_{col} > Sc = \nu/D_f \gg 1$, where Sc is the Schmidt number and D_f the self-diffusion constant of the fluid particles. Since $D_{col} < D_f$, the first inequality is always satisfied. When $Sc \approx 1$ momentum diffusion is dominated by mass diffusion, as in a gas. If $Sc \gg 1$ the fluid is liquidlike, the momentum diffusion is mainly mediated by collisions. To model a liquidlike system, we choose a relatively small collision interval ($\Delta t_c = 0.1a_0(m_f/k_B T)^{1/2}$), leading to $Sc \approx 5$. To prevent compressibility effects, the gravitational field g was limited such that $0.0067 \leq v_s/c_f \leq 0.1$, where $c_f = \sqrt{2k_B T/m_f}$ is the speed of sound in the fluid. Finally, to avoid large inertial effects, the particle Reynolds number $Re = v_s a/\nu$ should be $\ll 1$, as in real suspensions [1]. Inevitably there will be a compromise between computational efficiency and low Re . In our work $0.0016 \leq Re \leq 0.24$, depending on Pe , which is similar to the choice made for LB simulations [8,9].

To further test the accuracy of our method, we measured the Stokes drag F_d on the colloid for various values of the sphere radius σ_{cs} and gravitational field g . By varying the box size we find excellent agreement with analytic finite-size corrections [12], from which the infinite box-size limit extrapolates to $F_d = \gamma v_s = 4\pi\eta_f a v_s$, as expected for slip boundary conditions [10]. For the largest box sizes we compared the full velocity field around a single colloid to the known analytic result [1], and varied the ratio a_0/a , finding that errors scale roughly linearly with this parameter. We choose $a_0/a \approx \frac{1}{2}$, which leads to a relative error in the full velocity field of about 2%, similar to what is used in LB [8,9], and sufficiently accurate for the kinds of questions we investigate [11].

The sedimentation runs were performed in a periodic box of dimensions $L_x = L_y = 32a_0$ and $L_z = 96a_0$, with $N = 8-800$ colloids and $N_f \approx 5 \times 10^5$ SRD particles, corresponding to an average of about five particles per coarse-graining cell volume a_0^3 . The system size is similar

to some successful LB simulations [8]. A gravitational field g , applied in the z direction, was varied to produce different Pe . The simulations were run from 200 Stokes times t_S (for $Pe = 0.1$) to 30 000 t_S (for $Pe = 15$), where $t_S = a/v_s$ is the time it takes a sphere to sediment one particle radius. We verified that there was no drift in averages after about 100 t_S , so that the suspension is in steady state. To check that our system is large enough, we performed some runs for double the box size described above, as well as for $a_0/a = \frac{1}{4}$, finding no significant changes in our conclusions [11].

The average sedimentation velocity v_s for different Peclet numbers and different sphere packing fractions $\phi = \frac{4}{3}\pi\rho a^3$, with ρ the colloid number density, is shown in Fig. 1. At low densities the results are consistent with the Batchelor law [3], while at higher densities they compare well with a number of other forms also derived for the $Pe \rightarrow \infty$ limit [1]. Although one might naively expect that the effect of HI becomes weaker for $Pe < 1$, we observe that the results for *all* Peclet numbers $0.1 \leq Pe \leq 15$ lie exactly on the same curve. Taking into account only Brownian fluctuations gives $v_s = v_s^0(1 - \phi)$ [1], which heavily underestimates backflow effects. This is strong evidence that purely hydrodynamic arguments are still valid in an *average* sense at low Pe .

We next discuss velocity fluctuations around the average. In colloidal systems the instantaneous velocity fluctuations $\delta\mathbf{v} = \mathbf{v} - \mathbf{v}_s$ are dominated by thermal fluctuations, with a magnitude determined by equipartition: $\Delta v_T^2 = k_B T/m$. Here m is the mass of a colloid. To disentangle the hydrodynamic fluctuations from thermal fluctuations, we describe spatial and temporal correlations in the velocity fluctuations. The spatial correlation of the z component (parallel to the sedimentation) of the velocity fluctuations can be defined as

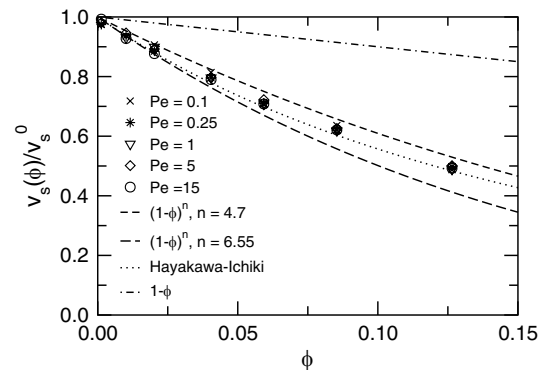


FIG. 1. Average sedimentation velocity, v_s normalized by the Stokes velocity v_s^0 , as a function of volume fraction ϕ for various Peclet numbers. The reduction of v_s due to hydrodynamic backflow effects is independent of Pe . Dashed lines correspond to two versions of the semiempirical Richardson-Zaki law $v_s/v_s^0 = (1 - \phi)^n$ [1]. The dotted line is another theoretical prediction taking higher order HI into account [17]. Ignoring hydrodynamics leads to $v_s/v_s^0 = 1 - \phi$ (dashed-dotted line).

$$C_z(\mathbf{r}) \equiv \langle \delta v_z(\mathbf{0}) \delta v_z(\mathbf{r}) \rangle, \quad (2)$$

where $\langle \dots \rangle$ represents a time average over many particles. The distance vector \mathbf{r} is taken perpendicular to sedimentation, $C_z(x)$, or parallel to it, $C_z(z)$. Similarly, the temporal correlation of the z component of the velocity fluctuations can be defined as

$$C_z(t) \equiv \langle \delta v_z(0) \delta v_z(t) \rangle, \quad (3)$$

where $\langle \dots \rangle$ represents a spatial average.

In Fig. 2 we plot $C_z(\mathbf{r})$, which shows a positive spatial correlation along the direction of flow, and an anticorrelation perpendicular to the flow, very much like that observed in experiments [13]. The inset of Fig. 2(a) shows that at $Pe = 1$ the correlation in the perpendicular direction, $C_z(x)$, is almost negligible compared with the thermal fluctuation strength $k_B T/m$, whereas for larger Pe , distinct regions of negative amplitude emerge, which grow with increasing Pe . Similarly, the inset of Fig. 2(b) shows correlations in the parallel direction that rapidly increase with Pe . For the highest Peclet numbers studied ($5 \leq Pe \leq 15$), the amplitudes of these correlations grow proportionally to v_s^2 , as shown in the main plots of Fig. 2. Unfortunately, because the division by v_s^2 amplifies the statistical noise, we are unable to verify whether this scaling persists for $Pe < 5$. The minimum in Fig. 2(a) is limited by the box size. We checked this by simulating larger systems: the correlation size increased linearly with box dimensions [11], as found

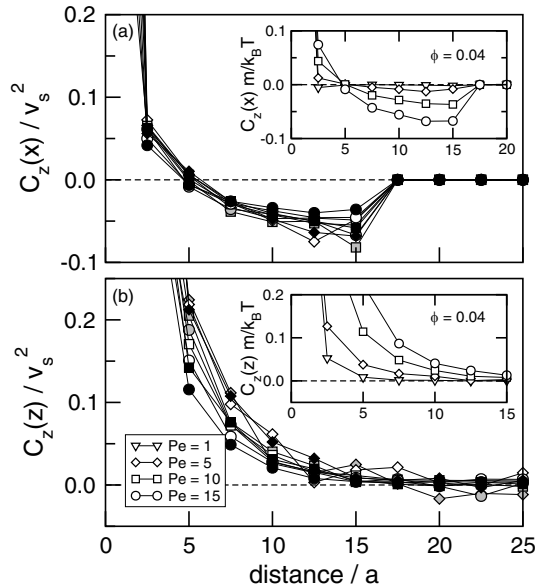


FIG. 2. Spatial correlation functions of the parallel (z) component of the velocity fluctuations as a function of distance perpendicular (a) and parallel (b) to the external field, for three different volume fractions [$\phi = 0.02$ (gray symbols), $\phi = 0.04$ (white), $\phi = 0.086$ (black)] and different Peclet numbers. The correlation functions are scaled with v_s^2 to emphasize hydrodynamic fluctuations. The insets show how $C_z(\mathbf{r})$, scaled with $C_z(0) = k_B T/m$, increases with Pe .

for LB [8], suggesting that the hydrodynamic velocity fluctuations are unscreened.

The following time scales are important for temporal correlations: In a liquid, the solvent relaxation time τ_f , typically of order 10^{-14} s [1], is the smallest relevant time scale. A (larger) Brownian particle experiences random forces and a friction γ . As a consequence, it loses memory of its initial velocity after a time $\tau_B \approx m/\gamma$, which is typically of the order of 10^{-9} s [1]. For time scales larger than τ_B , the particle experiences diffusive behavior and after a time $\tau_D = a^2/D \gg \tau_B$ it has traveled over its own radius. For correct coarse-grained temporal behavior, the time scales do not need to be identical to the underlying fluid, but it is important that they are clearly separated [9]. This is indeed the case for our choice of SRD parameters, where $\tau_f \approx \Delta t_c = 0.1$, $\tau_B \approx 2$, and $\tau_D \approx 200$ (in units $a_0(m_f/k_B T)^{1/2}$). Since the Stokes time $t_s \equiv a/v_s = \tau_D/Pe$ must be $\gg \tau_B$, this sets a limit on the maximum Pe number for these parameters.

Figure 3 shows the temporal correlation functions along the direction of sedimentation. At short times the behavior is well described by exponential Brownian relaxation [1]: $C_{\text{short}}(t) = \Delta v_T^2 \exp(-t/\tau_B)$. At intermediate times it follows the well known algebraic long-time tail $C_{\text{long}}(t) = Bt^{-3/2}$, associated with the fact that momen-

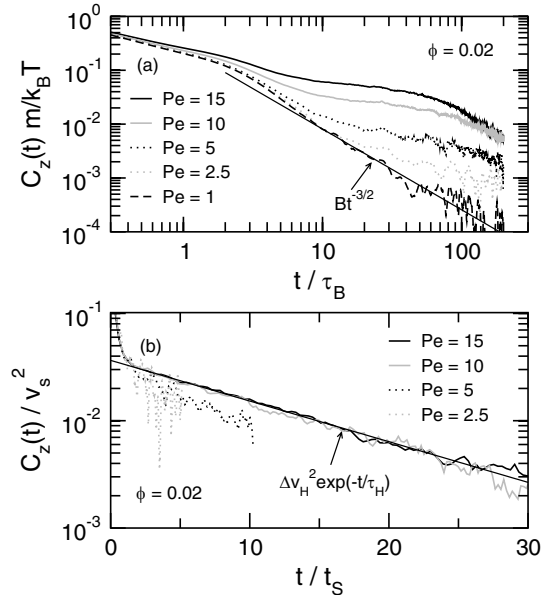


FIG. 3. Temporal correlation functions of the z component of the velocity fluctuations for $\phi = 0.02$ and different Peclet numbers. (a) Time is scaled with the Brownian relaxation time $\tau_B = m/\gamma$ and the velocities are scaled with the thermal fluctuation strength $k_B T/m$. The straight line is the hydrodynamic long-time tail $Bt^{-3/2}$ with $B^{-1} = 12\rho_f k_B T(\pi\nu)^{3/2}$ [14]. The results for $Pe \leq 1$ are indistinguishable. (b) Time is scaled with the Stokes time $t_s = a/v_s$ and $C_z(t)$ is scaled with v_s^2 to highlight hydrodynamic velocity fluctuations. The straight line is a fit demonstrating the exponential decay of nonequilibrium hydrodynamic fluctuations.

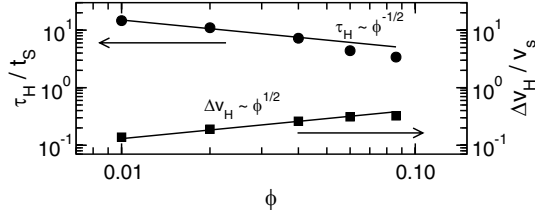


FIG. 4. Scaling of the hydrodynamic relaxation times (left scale) and velocity fluctuation amplitudes (right scale) with volume fraction. Straight lines are expected scalings for an unscreened system [4,15].

tum fluctuations diffuse away at a finite rate determined by the kinematic viscosity ν . Analytical *equilibrium* calculations of B [14] exactly fit the low Pe *nonequilibrium* results in Fig. 3(a) with no adjustable parameters!

Several experimental studies [13] on the sedimentation of non-Brownian ($Pe \rightarrow \infty$) particles have found an exponential relaxation of the form

$$C_z(t) = \Delta v_H^2 \exp(-t/\tau_H). \quad (4)$$

This nonequilibrium hydrodynamic effect takes place over much longer time scales than the initial exponential Brownian relaxation. The double-logarithmic Fig. 3(a) shows that a new mode of fluctuations becomes distinguishable in our simulations for $Pe > 1$. In Fig. 3(b) the correlation functions are scaled with v_s^2 to highlight the nonequilibrium hydrodynamic fluctuations. For $Pe \geq 10$ the fluctuations scale onto a single exponential master curve, similar to the high- Pe experiments [13], whereas for lower Pe deviations are seen. From the exponential fit to Eq. (4), we can estimate the relaxation time τ_H and the amplitude Δv_H^2 of the hydrodynamic fluctuations. These are shown in Fig. 4 for different volume fractions ϕ . The scalings of the relaxation time and fluctuation amplitude with ϕ are consistent with $\Delta v_H^2 \approx v_s^2 L \phi / (\frac{4}{3} \pi a)$ and $\tau_H^2 \approx L^2 / \Delta v_H^2 \approx t_s^2 \frac{4}{3} \pi L / (\phi a)$, predicted for unscreened hydrodynamic fluctuations by a simple heuristic argument [15] akin to that used by Caffish and Luke [4].

As seen in Fig. 3, the short time velocity fluctuations are dominated by thermal fluctuations at all Peclet numbers studied. By comparing Δv_H with Δv_T , we estimate the critical Pe^* , above which hydrodynamic fluctuations are larger than thermal fluctuations for all t [16]:

$$\frac{\Delta v_H}{\Delta v_T} \approx \frac{(k_B T L \phi \rho_c)^{1/2}}{\gamma} Pe \equiv \frac{Pe}{Pe^*}. \quad (5)$$

For example, for polystyrene colloids in water ($\eta = 10^{-3}$ Pa s, $T = 300$ K, $\rho_c = 1050$ kg m $^{-3}$), $Pe^* \approx [(a/10^{-14}\text{m})/(\phi L/a)]^{1/2}$. For $\phi = 0.001$, $a = 10^{-6}$ m, and $L/a = 100$ (smaller than the screening length at this concentration [13,16]), we find a large value: $Pe^* \approx 3 \times 10^4$.

In conclusion, we have adapted a mesoscopic simulation method, SRD [7], to study sedimentation at finite Peclet numbers. Hydrodynamic backflow corrections re-

duce the average sedimentation velocity v_s , irrespective of Pe . Thus, even when HI are relatively small, Brownian dynamics simulation methods [1] will yield qualitatively incorrect results for this problem. Long-time nonequilibrium velocity fluctuations become evident for $Pe > 1$, and scale like those for $Pe \rightarrow \infty$, while short time fluctuations are dominated by Brownian forces up to surprisingly large Pe . In other words, neither hydrodynamic interactions nor Brownian forces can be ignored for a significant parameter regime.

We thank R. Bruinsma, J. Dzubiella, J. Lister, and S. Ramaswamy for helpful discussions. J.T.P. thanks the EPSRC and IMPACT Faraday, and A. A. L. thanks the Royal Society (London) for financial support.

-
- [1] W.B. Russell, D.A. Saville, and W.R. Showalter, *Colloidal Dispersions* (Cambridge University Press, Cambridge, England, 1989); J.K.G. Dhont, *An Introduction to the Dynamics of Colloids* (Elsevier, Amsterdam, 1996).
 - [2] S. Ramaswamy, *Adv. Phys.* **50**, 297 (2001).
 - [3] G.K. Batchelor, *J. Fluid Mech.* **52**, 245 (1972).
 - [4] R.E. Caffish and J.H.C. Luke, *Phys. Fluids* **28**, 759 (1985).
 - [5] A. Levine, S. Ramaswamy, E. Frey, and R. Bruinsma, *Phys. Rev. Lett.* **81**, 5944 (1998).
 - [6] P.N. Segrè, F. Liu, P. Umbanhowar, and D.A. Weitz, *Nature (London)* **409**, 594 (2001).
 - [7] A. Malevanets and R. Kapral, *J. Chem. Phys.* **110**, 8605 (1999); T. Ihle and D.M. Kroll, *Phys. Rev. E* **67**, 066705 (2003); **67**, 066706 (2003); N. Kikuchi, C.M. Pooley, J.F. Ryder, and J.M. Yeomans, *J. Chem. Phys.* **119**, 6388 (2003).
 - [8] A.J.C. Ladd, *Phys. Rev. Lett.* **76**, 1392 (1996); **88**, 048301 (2002).
 - [9] M.E. Cates *et al.*, *J. Phys. Condens. Matter* **16**, S3903 (2004).
 - [10] Note that the SRD particles interact radially with the colloids, corresponding to slip boundary conditions. We do not expect any qualitative changes if we were to use no-slip boundary conditions.
 - [11] J.T. Padding and A. A. Louis (to be published).
 - [12] A. A. Zick and G.M. Homsy, *J. Fluid Mech.* **115**, 13 (1982).
 - [13] H. Nicolai *et al.*, *Phys. Fluids* **7**, 12 (1995); P.N. Segrè, E. Herbolzheimer, and P.M. Chaikin, *Phys. Rev. Lett.* **79**, 2574 (1997); G. Bernard-Michel *et al.*, *Phys. Fluids* **14**, 2339 (2002).
 - [14] M.H. Ernst, E.H. Hauge, and J.M.J. van Leeuwen, *Phys. Rev. Lett.* **25**, 1254 (1970).
 - [15] F.R. Cunha, G.C. Abade, A.J. Sousa, and E.J. Hinch, *J. Fluids Eng.* **124**, 957 (2002).
 - [16] When hydrodynamic fluctuations are screened [13], then L in Eq. (5) should be replaced by the screening length $\xi(a, \phi)$, which increases Pe^* .
 - [17] H. Hayakawa and K. Ichiki, *Phys. Rev. E* **51**, R3815 (1995).